Article

Synthesis and Anticancer Activity of Novel 9-*O*-Substituted Berberine Derivatives

Viktor Milata [1], Alexandra Svedova [2], Zuzana Barbierikova [3], Eva Holubkova [1], Ingrid Cipakova [4], Dana Cholujova [4], Jana Jakubikova [4], Miroslav Panik [5], Sona Jantova [2], Vlasta Brezova [3],* and Lubos Cipak [4],*

[1]   Institute of Organic Chemistry, Catalysis and Petrochemistry, Faculty of Chemical and Food Technology, Slovak University of Technology, Radlinskeho 9, 812 37 Bratislava, Slovakia; viktor.milata@stuba.sk (V.M.); evaholubicka@gmail.com (E.H.)

[2]   Institute of Biochemistry and Microbiology, Faculty of Chemical and Food Technology, Slovak University of Technology, Radlinskeho 9, 812 37 Bratislava, Slovakia; s.svedova@gmail.com (A.S.); sona.jantova@stuba.sk (S.J.)

[3]   Institute of Physical Chemistry and Chemical Physics, Faculty of Chemical and Food Technology, Slovak University of Technology in Bratislava, Radlinskeho 9, 812 37 Bratislava, Slovakia; zuzana.barbierikova@stuba.sk

[4]   Cancer Research Institute, Biomedical Research Center, University Science Park for Biomedicine, Slovak Academy of Sciences, Dubravska cesta 9, 845 05 Bratislava, Slovakia; ingrid.cipakova@savba.sk (I.C.); dana.cholujova@savba.sk (D.C.); jana.jakubikova@savba.sk (J.J.)

[5]   Institute of Management, Slovak University of Technology, 812 33 Bratislava, Slovakia; miroslav.panik@stuba.sk

*   Correspondence: vlasta.brezova@stuba.sk (V.B.); lubos.cipak@savba.sk (L.C.)

check for updates

Abstract: Berberine is a bioactive isoquinoline alkaloid derived from many plants. Although berberine has been shown to inhibit growth and induce apoptosis of several tumor cell lines, its poor absorption and moderate activity hamper its full therapeutic potential. Here, we describe the synthesis of a series of 9-*O*-substituted berberine derivatives with improved antiproliferative and apoptosis-inducing activities. An analysis of novel berberine derivatives by EPR spectroscopy confirmed their similar photosensitivity and analogous behavior upon UVA irradiation as berberine, supporting their potential to generate ROS. Improved antitumor activity of novel berberine derivatives was revealed by MTT assay, by flow cytometry and by detection of apoptotic DNA fragmentation and caspase-3 activation, respectively. We showed that novel berberine derivatives are potent inhibitors of growth of HeLa and HL-60 tumor cell lines with IC_{50} values ranging from 0.7 to 16.7 μM for HL-60 cells and 36 to >200 μM for HeLa cells after 48 h treatment. Further cell cycle analysis showed that the observed inhibition of growth of HL-60 cells treated with berberine derivatives was due to arresting these cells in the G_2/M and S phases. Most strikingly, we found that berberine derivative **3** (9-(3-bromopropoxy)-10-methoxy-5,6-dihydro-[1,3]dioxolo[4,5-g]isoquino[3,2-a] isoquinolin-7-ylium bromide) possesses 30-fold superior antiproliferative activity with an IC_{50} value of 0.7 μM and 6-fold higher apoptosis-inducing activity in HL-60 leukemia cells compared to berberine. Therefore, further studies are merited of the antitumor activity in leukemia cells of this berberine derivative.

Keywords: berberine; berberine derivatives; EPR spectroscopy; antitumor activity; cell cycle arrest; apoptosis

1. Introduction

Berberine is a well-known bioactive isoquinoline alkaloid present in a wide variety of medicinal plants such as *Berberis aristata*, *B. aquifolium*, *B. vulgaris*, *Hydrastis canadensis*, *Coptis chinensis* and many others [1–3]. It has been shown to be active in several diseases such as diabetes, diarrhea, hormonal disorder, coronary heart disease, obesity or hyperlipidemia [2]. Berberine has also shown promising antiprotozoal, antifungal and antimicrobial activities with a range of bacteria [4–6]. Furthermore, recent studies have shown that berberine exerts potent anticancer activity towards a variety of cancer cell types, such as colorectal, leukemia, prostate, lung, glioma, esophageal, and ovarian [7–13].

Detailed studies have shown that berberine can induce apoptosis of tumor cells through its modulation of activity of several pro-apoptotic and anti-apoptotic genes. For example, it alters the Bcl-2/Bax ratio and decreases the mitochondrial membrane potential of selected tumor cells [14]. In addition, it might induce apoptosis through the mitochondrial/caspase pathway, activate caspase-3, and caspase-8, and release the cytochrome *c* [3,8]. It has been also shown that berberine has a variety of effects on the cell cycle and its lower concentrations arrest tumor cells in the G_1 phase [15,16]. In contrast, higher concentrations of berberine induce the arrest of tumor cells in the G_2/M phase [17]. Interestingly, it has been reported that berberine might also induce apoptosis of tumor cells by a mechanism that involves the production of a reactive oxygen species (ROS) [18–21]. Most importantly, several reports have demonstrated that berberine could be combined with radiotherapy or chemotherapy drugs to neutralize their toxicity and enhance their therapeutic activities, thereby improving therapeutic outcomes [22–28].

Several studies have shown that berberine selectively inhibits tumor cell growth and induces apoptosis while eliciting less cytotoxic effects in normal cells [29,30]. Its poor absorption and moderate activity, however, hamper its full antitumor therapeutic potential [31]. As a result, many laboratories have focused their efforts towards the design and synthesis of novel berberine derivatives with improved biological activities, which has led to the synthesis of numerous berberine derivatives with various modifications at the C8, C9, C10, C12 and C13 positions of the berberine structure [32–38]. These studies have shown that modifications of berberine at C8 or C13 positions mainly increase its antimicrobial activity, which is closely related to the length of the substituent chains. On the other hand, the modifications to the C9 position of berberine usually increased its antitumor activities [39].

Over the past years, several novel 9-*O*-substituted berberine derivatives, including the 9-*O*-pyrazole alkyl group [40], 9-*O*-chlorohexyl group [41], or 9-*O*-alkyl- and 9-*O*-terpenyl group [35] modified berberine derivatives with improved aqueous solubility and enhanced absorption have been synthesized and tested for their anticancer activity. These studies have shown berberine derivatives to be more potent antitumor agents with improved apoptosis-inducing activity than that of berberine. Additionally, it has been shown that the substitution of berberine on C9 with lipophilic group substitutes, such as ibuprofen and naproxen [42], or cinnamic acid [36], significantly increased the anti-inflammatory and enhanced the hypoglycemic activity of berberine, respectively. These studies point out that modification of berberine on the C9 position can significantly improve its biological activities. Several recent reviews have summarized and outlined in more detail the most important findings on the relationship between various structural modifications of berberine and its improved pharmacological activities [38,43,44].

Here, we report the synthesis and evaluation of biological activity of four novel 9-*O*-substituted berberine derivatives. To improve the pharmacological properties and increase the therapeutic efficiency of berberine, we synthesized its 9-*O*-substituted derivatives bearing 2-chloro- and 2-bromo-acetoxy substituents (derivate **1** and **2**), 3-bromopropoxy substituent (derivate **3**) and ciprofloxacin (derivate **4**) (Figure 1, Schemes 1–5). Ciprofloxacin, as a quinolone antibiotic, was selected for the synthesis of berberine derivative **4** as it was reported to have high intrinsic lipophilicity [45] and various biological activity, including the activity against multidrug resistant bacteria *Klebsiella pneumoniae* [46,47].
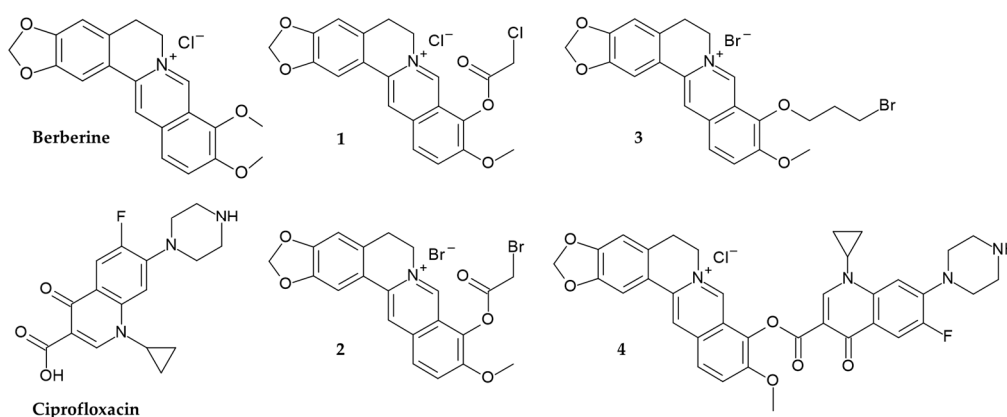
Figure 1. Chemical structures of berberine, ciprofloxacin and newly synthesized berberine derivatives.

We demonstrate that novel berberine derivatives maintain similar photosensitivity and analogous behavior upon UVA irradiation to that of berberine, supporting their potential to induce apoptosis through generation of the reactive oxygen species (ROS). We show that novel berberine derivatives are more potent antiproliferative and apoptosis-inducing agents compared to berberine. Moreover, these derivatives arrest HL-60 leukemia cells in the G_2/M and S phases, with the most promising derivative **3** showing superior apoptosis-inducing activity.

2. Results and Discussion

Berberine molecule offers a variety of possible modifications at positions C2, C3, C8, C9, C10, C12, C13 or C=N+ [32–38,48]. Based on previous reports that derivatization of berberine at the C9 position usually increases its antitumor activities [39], we prepared a set of novel 9-*O*-substituted berberine derivatives. Following the established procedures of heating the berberine to 190 °C for at least 15 min under vacuum [35] or under microwave irradiation [49,50], we performed selective demethylation of the berberine on its methoxy group at position C9 to obtain berberrubine (Scheme 1, see section Materials and Methods).

Berberrubine was then treated with 1,3-dibromopropane (DBP) to prepare the berberine derivative **3** (Scheme 3). No base was used here to avoid cyclisation to nitrogen. Various conditions for the synthesis of berberine derivative **3** were tested and obtained yields were summarized in Table 1.

Table 1. Reaction conditions for the preparation of berberine derivative **3** (1 equivalent of substrate, no base used).

Reaction	DBP (Equivalents)	Solvent	Temperature (°C)	Time (h)	Yield (%)
R_1	3	CH_3CN	60	2	48
R_2	10	CH_3CN	60	2	55
R_3	10	DMF	80	2	59
R_4	58	DMF	80	2	74

As presented, we found that the high excess of alkylating agent DBP was the most important factor in increasing the yield of the reaction. Similar to the alkylation of berberrubine by DBP, the excess of the haloacetylhalogenides was limiting factor for derivatization of berberrubine to haloacetylesters **1** and **2** (Scheme 2). It should be noted that, under these conditions, the separation of berberine derivatives from reactions was simple because the products were soluble in polar aprotic solvents, thus distinguishing them from the berberrubine. Concerning the synthesis of the berberine-ciprofloxacin conjugate (referred as berberine derivative **4**), the first step of its synthesis was the derivatization of ciprofloxacin to its acylated form (Scheme 4) [51,52]. Prepared carbonyl chloride of ciprofloxacin was further mixed with berberrubine and the reaction was microwave irradiated to produce the berberine derivative **4** in 31% yield (Scheme 5). Importantly, no berberine derivative **4** was obtained without

microwave irradiation. It is widely accepted that microwave irradiation is an unconventional energy source with great potential in synthetic organic chemistry [53]. In this respect, microwave irradiation has been applied with success to synthesize berberine derivatives under mild reaction conditions and with short reaction times [49,50,54].

The synthetic routes and characterization of novel berberine derivatives **1–4** by ^{1}H NMR and ^{13}C NMR spectroscopy are described in detail in the Materials and Methods section (Schemes 2–5).

It was previously shown that berberine, like many other bioactive molecules, exhibits sensitivity towards light and its photochemical behavior is strongly affected by the solvent and the presence of molecular oxygen [55]. As a photosensitive agent, berberine was previously studied, and the photoinduced generation of ROS, via both electron and energy transfer mechanisms (Types I and II), was evidenced by EPR spectroscopy and direct detection of singlet oxygen phosphorescence [20,56,57]. The investigation of the cytotoxic/phototoxic effect of berberine on murine fibroblast non-cancer NIH-3T3 and Ehrlich ascites carcinoma (EAC) cells showed a statistically significant degree of UVA induced increase of the cytotoxic effect only in cell line EAC. The cell cycle profile analysis revealed that the DNA damage triggered by berberine in combination with UVA irradiation led to a significant blockage of cells in the S and G_2/M phases with no sub-G_0 cell fraction detected [20]. Consequently, to provide a more complex view on the newly prepared berberine derivatives, their ability to produce ROS upon UVA irradiation (λ_{max} = 365 nm) was tested using the in situ EPR spin trapping technique.

The UV/vis absorption spectra of the prepared derivatives were recorded to follow the effect of the structural changes on the absorption maxima (Figure 2). We found that berberine derivative **3** exhibits an analogous spectrum to that of berberine with the characteristic absorption maxima at 348 nm and 421 nm (Figure 2B), while berberine derivatives **1** and **2** reveal a slight bathochromic shift of these bands (355 and 464 nm) together with the presence of other bands in the 300–600 nm region (Figure 2A). The absorption bands reaching higher wavelength up to 600 nm reflect the extended conjugation in berberine derivatives **1** and **2** due to the presence of 1-chloro-acetyl or 1-bromo-acetyl substituents. A combination of berberine with ciprofloxacin (berberine derivative **4**) led to a slight bathochromic shift of the absorption maxima (325 and 337 nm) compared to the ciprofloxacin (321 and 334 nm) and the appearance of broad shoulders at higher wavelength (370 and 490 nm), expanding the absorption more towards the visible region (Figure 2C). As novel berberine derivatives reveal a suitable overlap of their absorption spectra and the emission of UVA light, a source with a maximum at 365 nm was applied in further photochemical experiments.

The ROS generation initiated by UVA photoexcitation of berberine derivatives was investigated using indirect techniques of EPR spectroscopy. The application of spin trapping agent 5,5-dimethyl-1-pyrroline *N*-oxide (DMPO) enabled us to follow the formation of reactive radical intermediates upon in situ photoexcitation of berberine derivatives as the corresponding spin-adducts. The EPR spin trapping experiments confirmed that berberine derivatives preserved the photosensitivity of the parent berberine molecule, since they exhibited the photoinduced formation of DMPO spin-adducts upon UVA irradiation, reaching the highest EPR signal intensity for derivative **3** (Figure 3).
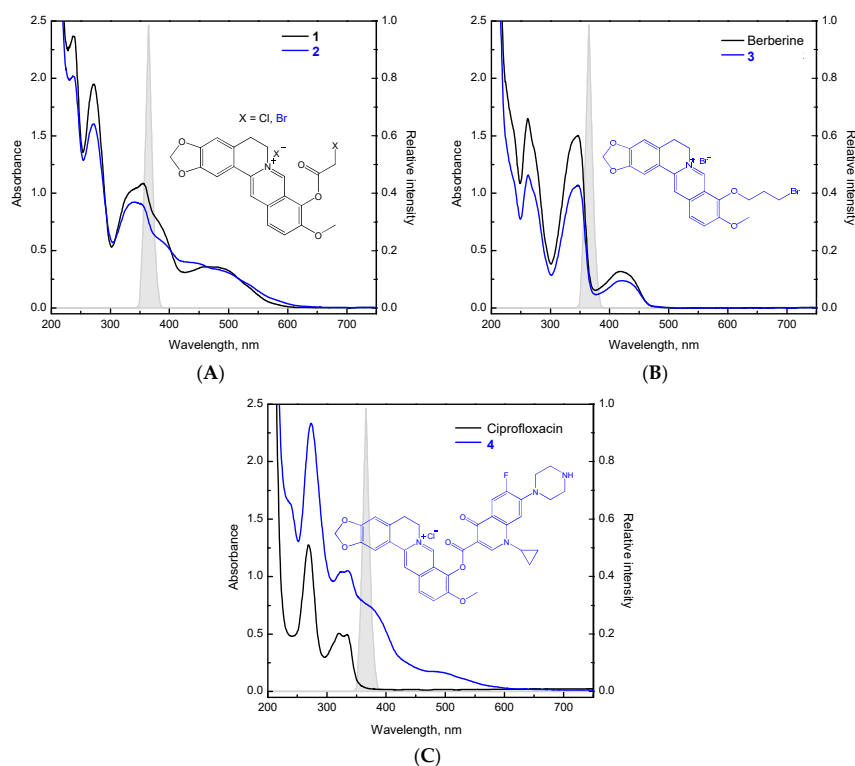
Figure 2. Electronic absorption spectra of (**A**) berberine derivatives **1** and **2**, (**B**) berberine and berberine derivative **3**, (**C**) ciprofloxacin and berberine derivative **4**, all in the mixed solvent DMSO/water (1:100, *v*:*v*; concentration 0.07 mM). Each graph contains the relative spectral distribution of the UVA LED source (λ_{max} = 365 nm) applied in the EPR spin trapping experiments.
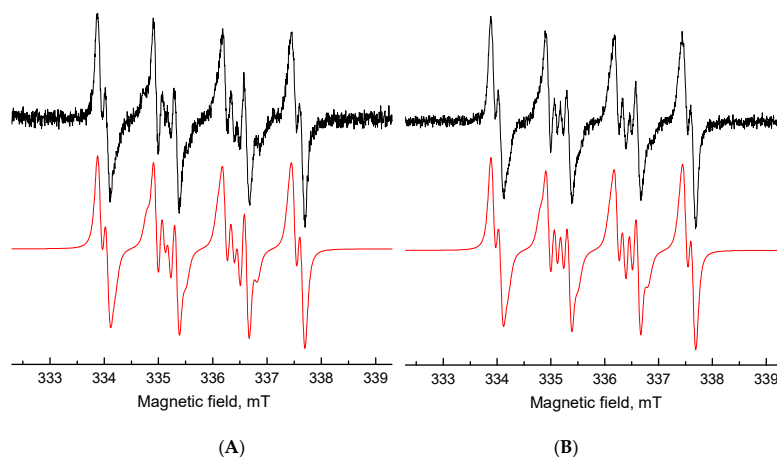

Figure 3. Experimental (–) and simulated (–) EPR spectra obtained after 13 min UVA exposure of the DMSO solution of (**A**) berberine and (**B**) berberine derivative **3** in the presence of DMPO spin trap under air. (Initial concentrations: c_0(berberine) = c_0(berberine derivative **3**) = 0.001 M, c_0(DMPO) = 0.042 M, λ_{max} = 365 nm, irradiance 13 mW·cm^{-2}).

The dominant twelve-line signal corresponding to berberine derivative **3** in the spectrum was assigned to the •DMPO-O$_2$$^-$ (spin-Hamiltonian parameters, a_N = 1.279 mT, a_H^β = 1.025 mT; a_H^γ = 0.137 mT; g = 2.0059) based on the simulation analysis. This evidences the effective electron transfer from the photoexcited berberine derivative **3** to the molecular oxygen generating the superoxide radical anion stabilized in the aprotic DMSO solvent. Further spin-adduct recognizable in the spectrum belongs to the spin-adduct •DMPO-OCH$_3$ (a_N = 1.303 mT, a_H^β = 0.842 mT; a_H^γ = 0.147 mT; g = 2.0059) originating from the •OCH$_3$ produced by the interaction of O$_2$•$^-$ with DMSO. Even though

the absorption of the berberine derivatives is shifted towards the visible region, only a negligible concentration of DMPO spin-adducts upon the visible-light irradiation ($\lambda > 420$ nm) was found.

The EPR spectra monitored during the continuous irradiation of the berberine and its derivatives **1–4** in a mixed water/DMSO (2:3, *v:v*) solvent containing DMPO are more complex and represent superposition of signals attributable to four individual DMPO spin-adducts, as shown in the berberine derivative **2** in Figure 4A. Based on the spin-Hamiltonian parameters elucidated from the simulation analysis, the signals were assigned to the spin-adducts ˙DMPO-O_2^-/O_2H ($a_N = 1.340$ mT, $a_H^\beta = 1.069$ mT; $a_H^\gamma = 0.131$ mT; $g = 2.0059$) and ˙DMPO-OH ($a_N = 1.433$ mT, $a_H^\beta = 1.303$ mT; $a_H^\gamma = 0.071$ mT; $g = 2.0057$) [58] and to the two spin-adducts of the carbon-centered radicals with slightly different parameters: ˙DMPO-CR1 ($a_N = 1.551$ mT, $a_H^\beta = 2.197$ mT; $g = 2.0056$) and ˙DMPO-CR2 ($a_N = 1.506$ mT, $a_H^\beta = 2.121$ mT; $g = 2.0057$). The last two spin-adducts were produced via interaction of photogenerated ROS with DMSO or berberine molecules. Moreover, a low-intensity single-line signal ($g \sim 2.0043$, asterisk in Figure 4A) with unresolved hyperfine structure was found upon UVA photoexcitation of the berberine derivative **2** in water/DMSO (2:3, *v:v*) solution under given experimental conditions, which was most probably produced by the electron transfer reactions of the photoexcited berberine derivative **2**, and its *g*-value is compatible with the oxygen-centered radicals [59]. The generation of this radical species was observed also upon continuous UVA irradiation of the aqueous solution of berberine derivative **2** in the presence of DMPO spin trap, along with the low-intensity four-line signal of ˙DMPO-OH spin-adduct ($a_N = 1.506$ mT, $a_H^\beta = 1.478$ mT; $g = 2.0057$) (Figure 4B).
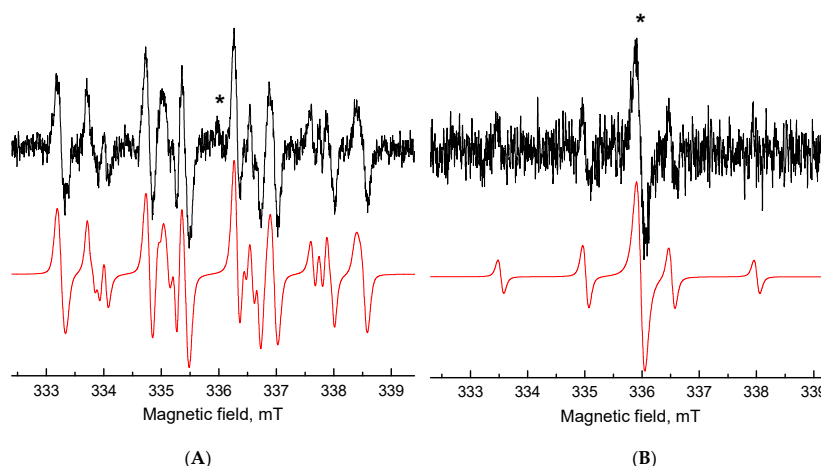

Figure 4. Experimental (**–**) and simulated (**–**) EPR spectra obtained after 13 min UVA exposure of berberine derivative **2** in the presence of DMPO spin trap under air in: (**A**) water/DMSO (2:3, *v:v*) and (**B**) water. (Initial concentrations: c_0(berberine derivative **2**) = 0.8 mM, c_0(DMPO) = 0.042 M, $\lambda_{max} = 365$ nm, irradiance 13 mW·cm^{-2}).

Upon the continuous UVA irradiation of berberine derivatives **1–4** in the presence of sterically-hindered amine 4-oxo-2,2,6,6-tetramethylpiperidine (TMPO) in DMSO, we only monitored the generation of low-intensity EPR signal of 4-oxo-2,2,6,6-tetramethylpiperidine *N*-oxyl (Tempone) produced via TMPO oxidation by singlet oxygen. The generated nitroxide radical Tempone is most likely transformed to the diamagnetic products by the interaction of >NO˙ moiety with other radical intermediates [60], effectively formed upon the UVA photoexcitation of berberine derivatives **1–4**.

Overall, the EPR spin trapping experiments demonstrated analogous behaviour of novel berberine derivatives upon UVA irradiation involving effective ROS generation to that of berberine. It will be interesting to examine these berberine derivatives for their dose-dependent accumulation of intracellular ROS to find out if generated ROS are involved in their cytotoxicity.

The antiproliferative activity of berberine derivatives was carried out by the 3-(4,5-dimethylthiazol-2-yl)-2,5-diphenyltetrazolium bromide (MTT) assay and rated in half-maximal inhibitory concentration, which is a measure of the effectiveness of an agent in inhibiting the growth and viability of cells [61]. The antiproliferative activity of berberine derivatives in tumor HeLa and HL-60 cell lines is summarized in Table 2.

Table 2. IC_{50} values (μM) for antiproliferative activity of berberine, ciprofloxacin and berberine derivatives **1–4** determined by MTT assay.

Cell Line	Time (h)	Berberine	Ciprofloxacin	1	2	3	4
HeLa	24	>200	>200	>200	>200	58 ± 2.6	>200
	48	126 ± 7.8	175 ± 8.7	115 ± 7.4	95 ± 4.8	36 ± 1.9	>200
HL-60	24	43.7 ± 1.1	>200	23.4 ± 2.6	14.6 ± 1.7	2.7 ± 0.9	19.3 ± 1.3
	48	27.1 ± 2.6	142 ± 5.7	16.7 ± 0.8	11.2 ± 1.6	0.7 ± 0.2	15.7 ± 1.9

We observed an increase in antiproliferative activity of berberine derivatives **1–4** against tested tumor cell lines compared to berberine or ciprofloxacin. Cytotoxic activity was observed in berberine derivatives **1**, **2** and **4** with IC_{50} values ranging from 95.0 to >200 μM for HeLa cells and from 11.2 to 23.4 μM for HL-60 cells. The lowest antiproliferative activity was found for berberine derivative **4** with IC_{50} values ranging from 15.7 to >200 μM. Most strikingly, the highest antiproliferative activity towards tested tumor cell lines was observed in berberine derivative **3** with IC_{50} values of 58.0 and 36.0 for HeLa cells and 3.7 and 0.7 μM for HL-60 cells treated for 24 and 48 h, respectively. This finding is in agreement with the previous study showing that 9-*O*-pyrazole alkyl substituted berberine derivatives have increased anticancer activity compared to berberine, with IC_{50} values ranging from 48.8 to 100.4 μM for HeLa cells after 24 h treatment [40].

The effect of berberine derivatives towards tumor HeLa and HL-60 cells was further assessed by analyzing their impact on the cellular morphology of cells treated for 24 and 48 h (Figure 5). As shown, untreated HeLa cells had normal epithelial morphology. In contrast, in some tumor cells, exposure to 10 μM concentrations of berberine or its derivatives **1**, **2** and **3** induced the formation of cell membrane blebbing after 24 and 48 h of treatment. However, HeLa cells treated with 10 μM concentrations of ciprofloxacin and berberine derivative **4** did not show any morphological changes. On the other hand, compared to untreated HL-60 cells, which have the rounded morphology characteristic of leukemia cells, the treatment of HL-60 cells with 10 μM concentrations of berberine, ciprofloxacin and berberine derivatives **1–4** resulted in profound formation of cell membrane blebs.

As cell membrane blebbing, observed in sub-population of berberine derivative-treated HeLa and HL-60 cells, is one of the defining features of apoptosis [62,63], next, we analyzed the potential of novel berberine derivatives to induce apoptosis. We compared their ability to induce apoptosis by employing DNA laddering and caspase-3 activation assays. As presented, after incubation of HL-60 cells with 10 μM concentrations of berberine derivatives for 48 h, only berberine derivative **3** treated HL-60 cells were positive for apoptotic DNA fragmentation (Figure 6A) and had active caspase-3 (Figure 6B). Comparing the intensities of apoptotic DNA fragmentation and activation of caspase-3 in HL-60 cells treated with 30 μM berberine and 10 μM berberine derivative **3**, berberine derivative **3** clearly exhibited 30-fold superiority to that of berberine.
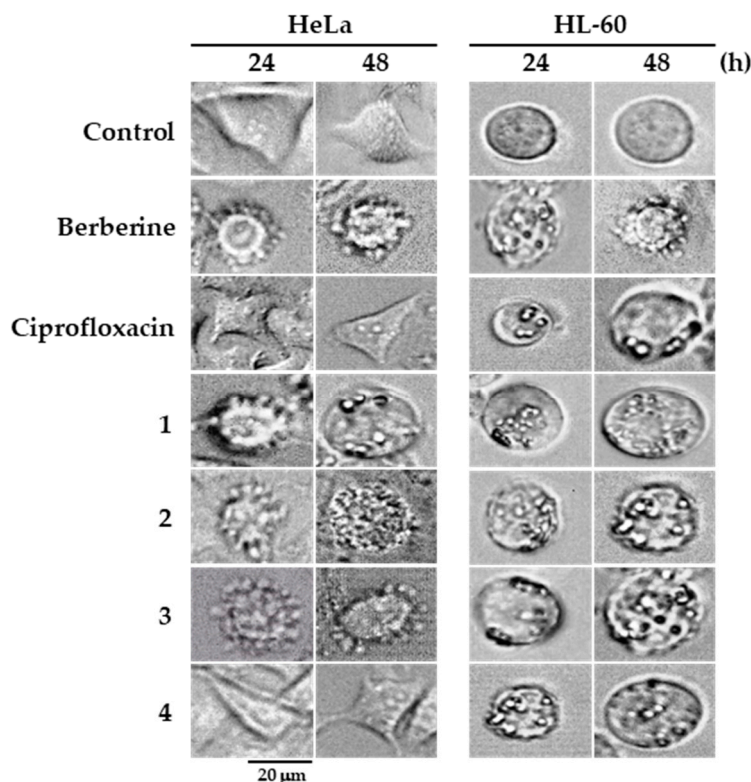
Figure 5. Assessment of changes in cellular morphology of HeLa and HL-60 cells treated with berberine, ciprofloxacin, and berberine derivatives (10 μM) for the time indicated. Magnification of microscope: ×600.
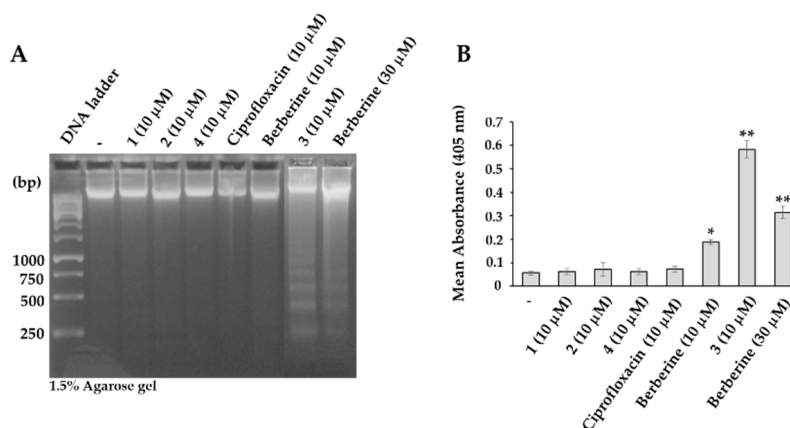

Figure 6. (**A**) Detection of apoptotic DNA fragmentation in HL-60 cells treated with indicated concentrations of berberine, ciprofloxacin and berberine derivatives for 48 h. (**B**) Activation of caspase-3 expressed as the mean absorbance at 405 nm (the relative amount of the pNA released from the DEVD-pNA). Each point represents a mean ± S.D. from 3 independent experiments. * $p < 0.05$, ** $p < 0.01$.

To further extend our cytotoxicity studies, we analyzed the effect of novel berberine derivatives on the cell cycle of HL-60 leukemia cells. We found that in contrast to berberine, which at 30 μM concentrations arrests HL-60 cells in the G_0/G_1 phase, the novel berberine derivatives **1** and **2** (30 μM) and **3** (10 μM) arrest HL-60 cells at the G_2/M phase with a proportional decrease of cells in the G_0/G_1 and S phases, while berberine derivative **4** induces G_2/M and S phases-arrest (Figure 7).
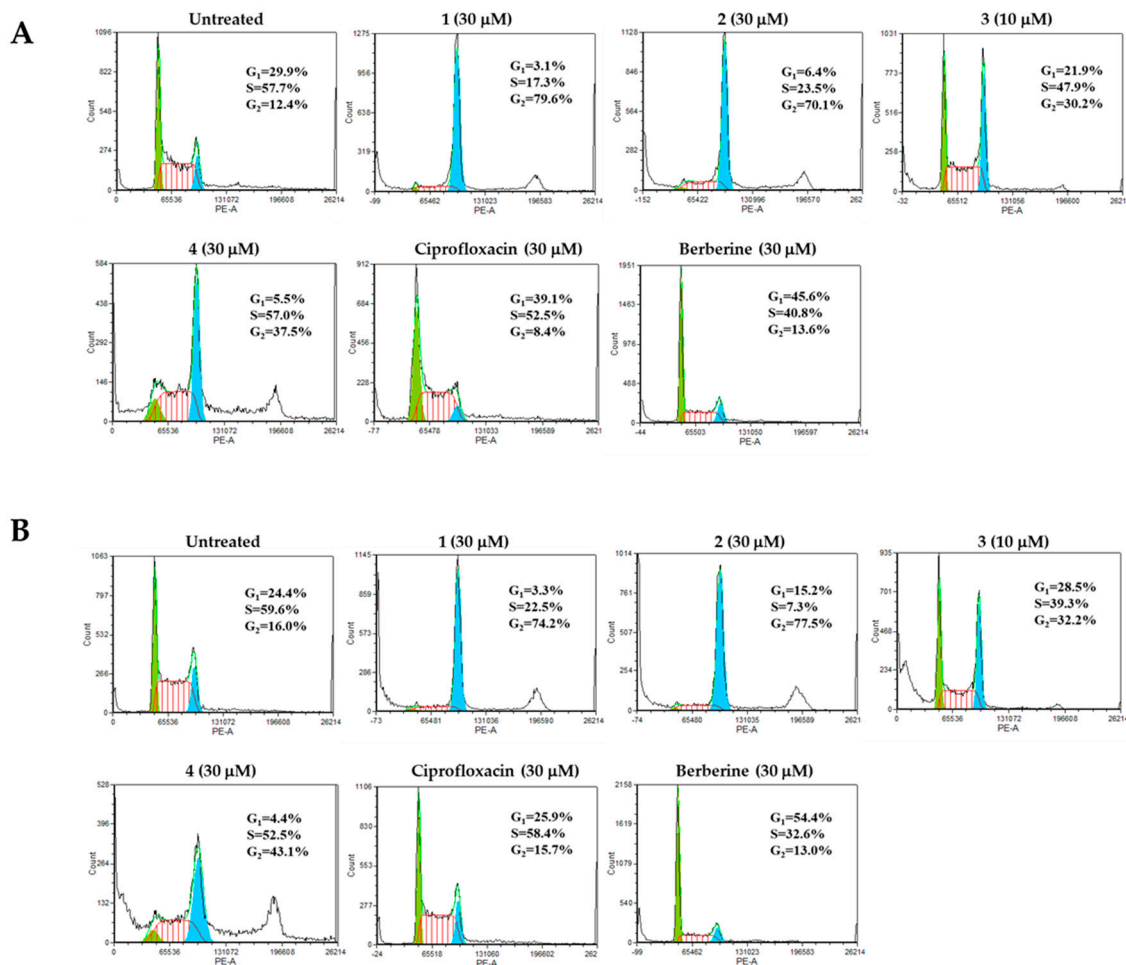
Figure 7. Analysis of cell cycle distribution of HL-60 cells treated with indicated concentrations of berberine, ciprofloxacin and berberine derivatives **1–4** for 24 h (**A**) and 48 h (**B**).

This finding indicates that novel berberine derivatives are more active molecules than berberine and ciprofloxacin, which in the same concentration have no effect or induce G_0/G_1 cell cycle arrest of HL-60 leukemia cells [15–17]. The observed G_2/M cell cycle arrest of HL-60 cells treated with berberine derivatives **1–4** supports their higher antiproliferative activity. Interestingly, berberine derivative **3** induced a significant increase in the number of cells defined as the sub-G_0 cell population (1.8% in untreated vs. 21.9% in berberine derivative **3** treated cells, Figure 7B), confirming its apoptotis-inducing potential.

In conclusion, we have synthesized a series of four novel 9-*O*-substituted berberine derivatives and evaluated their antiproliferative activity in human HeLa and HL-60 tumor cell lines. We found these derivatives to be more active antitumor agents than their parental molecules, berberine and ciprofloxacin. Most importantly, we showed that berberine derivative **3** (9-(3-bromopropoxy)-10-methoxy-5,6-dihydro-[1,3]dioxolo[4,5-g]isoquino[3,2-a]isoquinolin-7-ylium bromide) possesses the highest cytotoxic activity and ability to induce apoptosis of HL-60 leukemia cells. Therefore, this compound could become a promising candidate for anticancer therapy, and has been selected for the follow-up studies to reveal the molecular mechanisms of its antitumor action.

3. Materials and Methods

3.1. Experimental Methods

3.1.1. Chemistry

General

All reagents and solvents were purchased from Sigma-Aldrich® (Darmstadt, Germany), Alfa-Aesar® (Ward Hill, MA, USA), Fluka® (Buchs, Switzerland) and Mikrochem® (Pezinok, Slovakia). Solvents (acetonitrile, DMF, dioxane, THF) were purified and/or dried using standard laboratory methods and stored over molecular sieves (4 Å). Column chromatography was performed using silicagel Nomasil—40–63 μm (VWR®, Randor, PA, USA) and displayed eluent. Reaction progress was monitored by thin layer chromatography on Silufol or Alufol plates (Merck®, Darmstadt, Germany) with a UV indicator for λ = 254 nm.

Melting points (m. p.) of the prepared compounds were established on a Kofler block using digital thermometer TD 121 (VWR®, Randor, PA, USA).

Spectrometers INOVA 300 (300 MHz, 75 MHz, 282 MHz; Varian Inc., Palo Alto, CA, USA), VXR-300, Bruker (300 MHz, 75 MHz, Karlsruhe, Germany), and VNMRS 600 (600 MHz, 151 MHz, 564 MHz; Varian Inc., Palo Alto, CA, USA) were used for measurements of ^{1}H, ^{13}C and ^{19}F NMR spectra, at their frequencies at RT. Chemical shifts in (δ)–[ppm] (parts per million) were referenced to residual signal of the solvent. Coupling constants (J) were given in [Hz] with multiplicity: s (singlet), d (doublet), dd (doublet of the doublet), t (triplet), q (quartet), q (quintet) and m (multiplet).

Spectrometer Nicolet NEXUS 470 FT-IR (Thermo Fisher Scientific®, Madison, WI, USA) was used to obtain ATR IR absorption bands (ν) in [cm^{-1}]. High resolution mass spectra (HR-MS) were recorded with spectrometer LTQ Orbitrap XL (Thermo Fisher Scientific®, Madison, WI, USA). Microwave irradiation was realized in a CEM Discover microwave reactor (CEM Corporation, Matthews, NC, USA).

Selective Demethylation of Berberine on Its C9 Position

Berberine (2.0 g, 5.38 mmol) was placed into a round-bottomed flask equipped with a cross head magnetic stirrer. The flask was inserted into an oil bath preheated to 200 °C and attached to a vacuum pump. The berberine was then intensively stirred at 195 °C for 40 min (Scheme 1). After that, the obtained berberrubine was crystallized using a mixture of ethanol:methanol (1:1) by refluxing for 10 min. The obtained crystals of berberrubine were filtered using a Büchner funnel, washed with ethanol, and vacuum dried in a water bath at 40 °C.
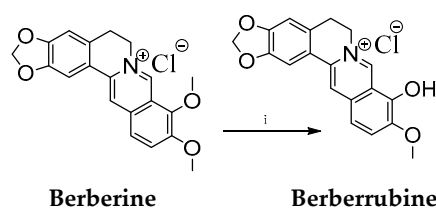
Scheme 1. Synthesis of berberrubine. Reaction conditions: (i) 195 °C (temperature of oil bath), 40 min.

The yield of berberrubine was 1.25 g (62.5%, red-brownish powder, m. p.: 275–279 °C).

^{1}H NMR: (CD$_3$OD) δ 9.28 (s, 1H, H-8), 8.70 (s, 1H, H-13), 7.54 (t, 1H, ^{3}J$_{HH}$ = 8.04 Hz, H-12), 7.49 (s, 1H, H-1), 6.91 (d, 1H, ^{3}J$_{HH}$ = 7.60 Hz, H-11), 6.85 (s, 1H, H-4), 6.04 (s, 2H, H-2′), 4.60 (t, 2H, ^{3}J$_{HH}$ = 5.32 Hz, H-6), 3.89 (s, 3H, H-10′), 3.12 (t, 2H, ^{3}J$_{HH}$ = 5.46 Hz, H-5).

^{13}C NMR: (CD$_3$OD) δ 149.5 (C-13′), 149.4 (C-9), 148.0 (C-10), 145.9 (C-8), 134.2 (C-2), 132.2 (C-3), 129.2 (C-12′), 122.6 (C-8′), 121.4 (C-4′), 120.1 (C-13″), 118.3 (C-12), 107.7 (C-11), 107.1 (C-13), 104.4 (C-4), 101.8 (C-1), 56.9 (C-2′), 55.2 (C-10′), 54.1 (C-6), 27.5 (C-5).

Synthesis of 9-(2-Chloro- or Bromo-acetoxy)-10-metoxy-5,6-dihydro-[1,3]dioxolo[4,5-g]isoquino[3,2-a] isoquinoline-7-ylium Chloride or Bromide

Berberrubine (0.7 g, 1.96 mmol) was dissolved in dry CH_3CN and stirred at 40 °C for 15 min. After that, haloacetylhalides chloracetyl chloride (0.29 mL, 2.55 mmol) or bromacetyl bromide (0.22 mL, 2.55 mmol) were dropped into the stirred reaction mixture, followed by stirring for additional 2 h. After cooling the mixture to RT, the products were filtered off, washed with dry CH_3CN and left to dry in a vacuum.
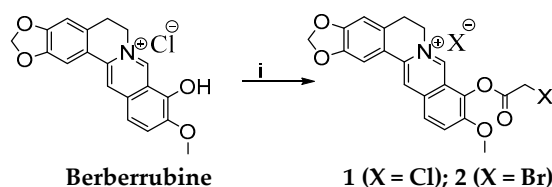
Scheme 2. Synthesis of berberine derivative **1** and derivative **2**. Reagents and conditions: (i) CH_3CN, 40 °C, 15 min, $C_2H_2Cl_2O$/$C_2H_2Br_2O$, 2 h.

The yield of berberine derivative **1** was 0.42 g (49%, yellow powder, m. p. > 300 °C).

^{1}H NMR: (CD_3OD) δ 10.03 (s, 1H, H-8), 8.72 (s, 1H, H-13), 8.54 (d, 1H, $^3J_{HH}$ = 8.05 Hz, H-11), 8.19 (d, 1H, $^3J_{HH}$ = 8.61 Hz, H-12), 7.27 (s, 1H, H-1), 7.16 (s, 1H, H-4), 6.34 (s, 2H, H-2′), 5.12 (t, 2H, $^3J_{HH}$ = 5.55 Hz, H-6), 4.19 (s, 2H, H-9″), 3.78 (s, 3H, H-10′), 3.14 (t, 2H, $^3J_{HH}$ = 5.34 Hz, H-5).

^{13}C NMR: (CD_3OD) δ 159.8 (C-9′), 152.6 (C-10), 147.9 (C-3), 147.1 (C-2), 146.3 (C-8), 140.1 (C-9), 135.5 (C-13′), 132.2 (C-12′), 131.9 (C-4′), 124.4 (C-11), 121.8 (C-12), 120.1 (C-8′), 119.1 (C-13″), 118.2 (C-13), 106.7 (C-4), 105.1 (C-1), 100.3 (C-2′), 61.1 (C-10′), 53.8 (C-6), 44.7 (C-9″) 21.77 (C-5).
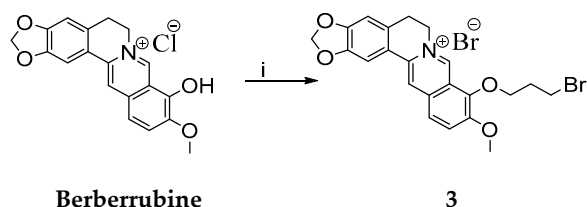
The yield of berberine derivative **2** was 0.38 g (38%, yellow-orange powder, m. p. > 300 °C).

^{1}H NMR: (CD_3OD) δ 9.83 (s, 1H, H-8), 8.71 (s, 1H, H-13), 8.64 (d, 1H, $^3J_{HH}$ = 8.15 Hz, H-11), 7.87 (d, 1H, $^3J_{HH}$ = 8.25 Hz, H-12), 7.23 (s, 1H, H-1), 7.14 (s, 1H, H-4), 6.72 (s, 2H, H-2′), 5.13 (t, 2H, $^3J_{HH}$ = 5.74 Hz, H-6), 4.22 (s, 2H, H-9″), 3.92 (s, 3H, H-10′), 3.03 (t, 2H, $^3J_{HH}$ = 5.21 Hz, H-5).

^{13}C NMR: (CD_3OD) δ 161.3 (C-9′), 149.2 (C-10), 148.1 (C-3), 145.7(C-2), 143.1 (C-8), 142.6 (C-9), 138.4 (C-13′), 134.8 (C-12′), 131.6 (C-4′), 129.1 (C-11), 123.3 (C-12), 122.7 (C-8′), 120.1 (C-13″), 117.8 (C-13), 109.2 (C-4), 107.4 (C-1), 100.9 (C-2′), 63.1 (C-10′), 52.5 (C-6), 45.9 (C-9″) 23.8 (C-5).

Synthesis of 9-(3-Bromopropoxy)-10-methoxy-5,6-dihydro-[1,3]dioxolo[4,5-g]isoquino[3,2-a] isoquinolin-7-ylium Bromide

Berberrubine (0.5 g, 1.40 mmol) was dissolved in dry DMF (10 mL) at 80 °C and stirred for 15 min. Then, 1,3-dibromopropane (8.2 mL, 80.75 mmol) was added dropwise and the reaction was stirred for 2 h. After cooling to RT, the diethyl ether (20 mL) was added. Separated precipitate was filtered off using Büchner funnel. Obtained berberine derivative **3** was further purified using column chromatography (eluent $CHCl_3$:MeOH—10:1).

Scheme 3. Synthesis of berberine derivative **3**. Reagents and conditions: (i) $C_3H_6Br_2$, DMF, 80 °C, 2 h.

The yield of berberine derivative **3** was 0.54 g (74%, yellow powder, m. p. > 300 °C).

^{1}H NMR: (CD_3OD) δ 9.79 (s, 1H, H-8), 8.94 (s, 1H, H-13), 8.20 (d, 1H, $^3J_{HH}$ = 8.25 Hz, H-11), 8.00 (d, 1H, $^3J_{HH}$ = 8.25 Hz, H-12), 7.79 (s, 1H, H-1), 7.09 (s, 1H, H-4), 6.17 (s, 2H, H-2′), 4.94 (t, 2H,

^{3}J$_{HH}$ = 5.98 Hz, H-6), 4.42 (t, 2H, ^{3}J$_{HH}$ = 9.28 Hz, H-9′), 4.06 (s, 3H, H-10′), 3.94 (t, 2H, H-9‴), 3.21 (t, 2H, ^{3}J$_{HH}$ = 5.58 Hz, H-5), 2.33 (p, 2H, H-9″).

^{13}C NMR: (CD$_3$OD) δ 150.2 (C-10), 149.8 (C-3), 147.6 (C-2), 145.2 (C-8), 142.4 (C-9), 137.5 (C-13′), 133.0 (C-12′), 130.7 (C-4′), 126.7 (C-11), 123.5 (C-12), 121.4 (C-8′), 120.4 (C-13″), 120.2 (C-13), 108.4 (C-4), 105.4 (C-1), 102.0 (C-2′), 71.2 (C-9′), 57.1 (C-10′), 55.2 (C-6), 42.1 (C-9‴), 32.6 (C-9″), 26.3 (C-5).

Synthesis of 1-Cyclopropyl-6-fluoro-4-oxo-7-piperazin-1-yl-1,4-dihydroquinoline-3-carbonyl Chloride

A round bottomed flask (equipped with Dimroth condenser and calcium chloride tube) containing thionyl chloride (0.85 mL, 11.7 mmol) was cooled in ice bath and the apparatus was filled with argon. After cooling off the flask content, ciprofloxacin (0.1 g, 0.3 mmol) was added. The colour of the suspension turned orange. The sample was stirred for 2 h. During stirring, the temperature was allowed to reach RT. Then dry CH$_2$Cl$_2$ (20 mL) was slowly added and the suspension was allowed to exsiccate until dry using a rotary vacuum evaporator. The procedure was repeated 3 times to remove the excess of HCl and thionyl chloride. As the result, the target carbonyl chloride derived from ciprofloxacin **5** was obtained [42].
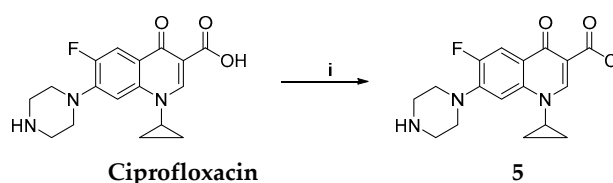
Ciprofloxacin　　　　　　　　　**5**

Scheme 4. Synthesis of chlorinated ciprofloxacin **5**. Reagents and conditions: (i) SOCl$_2$, RT, 2 h.

The yield of chlorinated ciprofloxacin **5** was 0.085 g (81%, red powder, m. p. 246–247 °C).

^{1}H NMR: (TFA-d) δ 9.63 (s, 1H, H-2), 9.47 (d, 1H, ^{3}J$_{HF}$ = 12.92 Hz, H-5), 8.13 (d, 1H, ^{4}J$_{HF}$ = 5.36 Hz, H-8), 3.93–4.49 (m, 5H, H-10, H-14, H-1′), 3.13 (t, 4H, ^{3}J$_{HH}$ = 4.71 Hz, H-11, H-13), 2.43 (s, 1H, H-12), 1.47–1.85 (m, 4H, H-1′, H-1″).

^{13}C NMR: (TFA-d) δ 178.2 (C-4), 162.3 (C-3′), 155.4 (C-2), 149.9 (C-6), 149.5 (C-7), 148.1 (C-8′), 117.2 (C-3), 115.1 (C-4′), 112.8 (C-5), 107.6 (C-8), 52.1, 52.3 (C-10, C-14), 44.6, 44.9 (C-11, C-13), 32.6 (C-1′), 12.6, 12.8 (C-1″, C-1‴).

^{19}F NMR: (TFA-d) δ −77.95 (F-6).

Synthesis of 9-(1-Cyclopropyl-6-fluoro-4-oxo-7-piperazin-1-yl-1,4-dihydroquinoline-3-carbonyloxy)-10-methoxy-5,6-dihydro-[1,3]dioxolo[4,5-g]isoquino[3,2-a]isoquinolin-7-ylium Chloride

During continuous stirring, berberrubine (0.071 g, 0.19 mmol) and NaH (0.03 g, 1.14 mmol) and after 15 min chlorinated ciprofloxacin **5** (0.07 g, 0.19 mmol) were slowly added to dry dioxane (5 mL). The reaction mixture was then irradiated for 10 min using 300 W power at a temperature of 100 °C. After cooling, the mixture was exsiccated until dry and further purified using column chromatography on silicagel using MeOH:CHCl$_3$ (1:10) as an eluent.

5　　　　　　　　　　　　　　　**4**
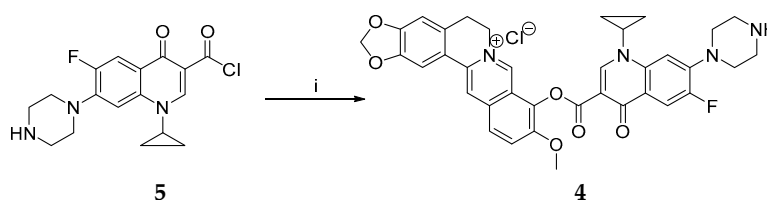
Scheme 5. Synthesis of berberine derivative **4**. Reagents and conditions: (i) berberrubine, NaH, dioxane, 300 W, 100 °C, 10 min.

The yield of berberrubine-ciprofloxacin conjugate, also referred to as berberine derivative **4** was 0.039 g (31%, dark brown powder, m. p. > 300 °C).

^{1}H NMR: (TFA-d) δ 9.43 (s, 1H, H-8), 9.31 (s, 1H, H-2C), 8.98 (d, 1H, $^3J_{HF}$ = 13.83 Hz, C-5C), 8.47 (d, 1H, $^3J_{HF}$ = 5.15 Hz, H-8C), 8.27 (d, 1H, $^3J_{HH}$ = 8.73 Hz, H-11), 7.98–8.12 (m, 3H, H-1, H-4, H-12), 6.63 (s, 2H, H-2'), 5.28 (t, 2H, $^3J_{HH}$ = 6.02 Hz, H-6), 4.25 (s, 3H, H-10'), 3.25–4.18 (m, 11H, H-5, H-10C, H-11C, H-13C, H-14C, H-1'C), 2.98 (s, 1H, H-12C), 1.53–1.72 (m, 4H, H-1''C, H-1'''C).

^{13}C NMR: (TFA-d) δ 176.1 (C-4C), 167.5 (C-3'C), 159.7 (C-2C), 152.6 (C-10), 151.7 (C-6C), 150.3 (C-7C), 148.1 (C-3), 146.9 (C-2), 144.9 (C-8), 143.5, 144.1 (C-9, C-8'), 140.0 (C-13'), 135.1 (C-12'), 131.7 (C-4'), 123.8 (C-11), 123.1 (C-12), 119.3, 120.7, 121.9 (C-8', C-13'', C-3C), 118.5 (C-13), 115.4 (C-8C), 106.3, 106.9, 108.2 (C-1, C-4, C-8C), 100.1 (C-2'), 62.1 (C-10'), 53.8, 54.6, 55.1 (C-6, C-10C, C-14C), 48.7, 49.3 (C-11, C-13), 38.7 (C-1'C), 31.4 (C-5), 14.7, 14.9 (C-1'', C-1''').

^{19}F NMR: (TFA-d) δ −75.71 (F6).

HRMS (ESI): calculated for $C_{36}H_{32}ClFN_4O_6$ (M + H$^+$): 671.1994; found: 670.9106.

3.1.2. Electron Paramagnetic Resonance (EPR) Spectroscopy Studies of Berberine Derivatives

The UV/visible spectra of berberine, ciprofloxacin and newly synthesized berberine derivatives dissolved in the mixed solvent DMSO/water (1:100, *v:v*) were recorded using a UV-3600 UV-vis-NIR spectrophotometer (Shimadzu, Kyoto, Japan) with a 1-cm square quartz cell.

The formation of paramagnetic intermediates of the studied berberine derivatives upon their UVA irradiation was monitored in situ using the EPR spin trapping technique. The photoinduced production of singlet oxygen during the excitation of berberine derivatives was followed by the oxidation of a sterically-hindered amine 4-oxo-2,2,6,6-tetramethylpiperidine (TMPO). The solution of the berberine derivatives was mixed either with the spin trapping agent 5,5-dimethyl-1-pyrroline N-oxide (DMPO) or TMPO solution, and immediately after a careful air or argon saturation using a slight gas stream, the prepared sample was transferred to a small quartz flat cell (WG 808-Q, optical cell length 0.04 cm; Wilmad-LabGlass, Vineland, NJ, USA) optimized for the TE102 cavity (Bruker, Rheinstetten, Germany) of the X-band EPR spectrometer (EMX Plus, Bruker, Rheinstetten, Germany). The photoexcitation of the samples took place directly in the EPR resonator at 295 K and the EPR spectra were recorded in situ during the continuous irradiation or after a defined exposure. A UV LED monochromatic radiator (λ_{max} = 365 nm; Bluepoint LED, Hönle UV Technology, Gräfelfing/München, Germany) reaching the irradiance value of 13 mW·cm^{-2} within the EPR cavity, determined using a UVX radiometer (UVP, Upland, CA, USA) or the visible-light source (KL 1600LED (T = 5600 K; Schott)) were used as the irradiation sources. The *g*-values were determined using a built-in nuclear magnetic resonance teslameter (ER 036TM, Bruker) and an integrated frequency counter. The EPR spectra were analyzed and simulated using Bruker software WinEPR and EasySpin toolbox working under Matlab software (MathWorks, Natick, MA, USA) [64].

3.1.3. Evaluation of Antiproliferative Activities of Berberine Derivatives

Cell Cultures and Determination of Cell Viability and Morphology

HL-60 (human promyelocytic leukemia) and HeLa (human cervix epithelioid carcinoma) cells were grown in a humidified atmosphere containing 5% CO_2 and 95% air at 37 °C. HeLa cells were maintained in a DMEM medium and HL-60 cells were maintained in RPMI 1640 medium, both supplemented with 10% (*v/v*) heat-inactivated fetal bovine serum (FBS), 50 U/mL penicillin, and 50 µg/mL streptomycin. Stock solutions of berberine and its derivatives were prepared in DMSO, except for a stock solution of ciprofloxacin, which was prepared in 0.1 M HCl. In all experiments, the final concentration of DMSO was kept ≤ 0.1% (*v/v*) and 0.1% DMSO alone was used as vehicle control. Cell viability was determined using a 3-(4,5-dimethylthiazol-2-yl)-2, 5-diphenyltetrazolium bromide (MTT) assay [61]. HL-60 cells (2×10^4 cells/well) or HeLa cells (4×10^4 cells/well) were seeded in 96-well plates. Cells were treated with various concentrations of berberine, ciprofloxacin and berberine derivatives (0–100 µM) for 24 and 48 h. At the end of the treatment, MTT solution (final concentration 1 mg/mL) was added to each well and the plates were incubated for another 4 h. The

precipitated formazan was dissolved in DMSO and its concentration was measured at 595 nm using a microplate reader (xMark, BioRad, Tokyo, Japan). Based on the curve fitting using nonlinear regression (Origin 7.0, Microcal), the median inhibitory concentrations IC_{50} values (the concentration resulting in 50% inhibition of the cell proliferation that was recorded in control experiments) were determined separately for each experiment. The values were calculated from three independent experiments. Data are presented as a mean $\pm$ SD ($n = 3$).

The morphology of cells treated with tested drugs was evaluated using light microscopy (Zeiss Jenalumar, Jena, Germany) [65].

Detection of Induction of Apoptosis by DNA Laddering Assay

Cells (2×10^6) treated with various concentrations of tested derivatives were washed with ice-cold PBS containing 10 mM EDTA. Pellets of cells were resuspended in 250 μL of lysis buffer (10 mM Tris-HCl, pH 8.0, 100 mM NaCl, 5 mM EDTA, 5% Triton-X, 0.25% SDS) supplemented with 0.4 mg/mL DNase-free RNase A, incubated at 65 °C for 15 min, cooled to RT for 10 min, and incubated at 37 °C for 90 min. After that, Proteinase K was added to a final concentration of 0.2 mg/mL and samples were incubated at 50 °C for an additional 1 h. The DNA was extracted with 200 μL of phenol:chloroform:isoamyl alcohol (25:24:1) for 1 min and centrifuged at 14,500$\times$ *g* for 5 min. The DNA was precipitated from the aqueous phase with 3 volumes of chilled EtOH containing 0.3 M sodium acetate. The DNA pellets were washed with 70% EtOH, dried, and dissolved in 100 μL of TE buffer. The DNA was separated on 1.5% agarose gel and visualized under UV illumination after being stained with GelRed Nucleic Acid Gel Stain (254 nm, Ultra-Lum Electronic UV Transilluminator, Paramount, CA, USA) [66].

Detection of Apoptosis by Caspase-3 Assay

Activation of caspase-3 was measured using a colorimetric caspase-3 assay kit (CaspACE^{TM} Assay System, Promega, Madison, WI, USA). Briefly, exponentially growing HL-60 cells were treated with tested derivatives (10–30 μM) for 48 h. Cells (5×10^6) were pelleted by centrifugation (1200$\times$ *g*, 3 min at 4 °C) and resuspended in 50 μL of lysis buffer (Promega, Madison, WI, USA). The lysed cell mixture was then incubated on ice for 15 min before centrifugation (13,000$\times$ *g*, 5 min at 4 °C). 42 μL of reaction buffer supplemented with 10 mM DTT were mixed with 20 μL of cell lysates. The substrate DEVD-pNA (2 μL) was added and the samples were incubated for 4 h at 37 °C. The release of *p*-nitroaniline from specific caspase-3 substrate was measured at 405 nm using a microplate reader (xMark, BioRad, Tokyo, Japan).

Determination of Cell Cycle Distribution

Cells (0.5×10^6) treated with berberine derivatives (0–30 μM) for 24 and 48 h were washed with PBS and fixed in ice-cold 70% ethanol. Next, the cells were washed twice with PBS and resuspended in 0.1% Triton-X in PBS containing 50 μg/mL RNase A and incubated for 30 min at 37 °C. Afterwards, DNA was stained using PI (50 μg/mL) for 15 min at 4 °C. The cell cycle distribution was analyzed using a FACS Canto II flow cytometer (Becton Dickinson, Franklin Lakes, NJ, USA). A minimum of 10,000 cells per sample was analyzed at a flow rate of 200 cells/s [67].

Conflicts of Interest: The authors declare no conflict of interest. The funders had no role in the design of the study; in the collection, analyses, or interpretation of data; in the writing of the manuscript, or in the decision to publish the results.

Abbreviations

DBP	1,3-Dibromopropane
DMF	Dimethylformamide
DMPO	5,5-Dimethyl-1-pyrroline *N*-oxide
DMSO	Dimethyl Sulfoxide
DTT	Dithiothreitol
MTT	3-(4,5-Dimethylthiazol-2-yl)-2,5-diphenyltetrazolium bromide
PBS	Phosphate buffer saline
PI	Propidium iodide
ROS	Reactive Oxygen Species
RT	Room temperature
Tempone	4-Oxo-2,2,6,6-tetramethylpiperidine *N*-oxyl
THF	Tetrahydrofuran
TMPO	4-Oxo-2,2,6,6-tetramethylpiperidine

References

1. Sun, Y.; Xun, K.; Wang, Y.; Chen, X. A systematic review of the anticancer properties of berberine, a natural product from Chinese herbs. *Anticancer Drugs* **2009**, *20*, 757–769. [CrossRef]
2. Tillhon, M.; Guamán Ortiz, L.M.; Lombardi, P.; Scovassi, A.I. Berberine: New perspectives for old remedies. *Biochem. Pharmacol.* **2012**, *84*, 1260–1267. [CrossRef]
3. Liu, D.; Meng, X.; Wu, D.; Qiu, Z.; Luo, H. A natural isoquinoline alkaloid with antitumor activity: Studies of the biological activities of berberine. *Front. Pharmacol.* **2019**, *10*, 9. [CrossRef]
4. Freile, M.L.; Giannini, F.; Pucci, G.; Sturniolo, A.; Rodero, L.; Pucci, O.; Balzareti, V.; Enriz, R.D. Antimicrobial activity of aqueous extracts and of berberine isolated from Berberis heterophylla. *Fitoterapia* **2003**, *74*, 702–705. [CrossRef]
5. Domadia, P.N.; Bhunia, A.; Sivaraman, J.; Swarup, S.; Dasgupta, D. Berberine targets assembly of *Escherichia coli* cell division protein FtsZ. *Biochemistry* **2008**, *47*, 3225–3234. [CrossRef]
6. Huang, Y.Q.; Huang, G.R.; Wu, M.H.; Tang, H.Y.; Huang, Z.S.; Zhou, X.H.; Yu, W.Q.; Su, J.W.; Mo, X.Q.; Chen, B.P.; et al. Inhibitory effects of emodin, baicalin, schizandrin and berberine on hefA gene: Treatment of Helicobacter pylori-induced multidrug resistance. *World J. Gastroenterol.* **2015**, *21*, 4225–4231. [CrossRef]
7. Guamán-Ortiz, L.M.; Croce, A.L.; Aredia, F.; Sapienza, S.; Fiorillo, G.; Syeda, T.M.; Buzzetti, F.; Lombardi, P.; Scovassi, A.I. Effect of new berberine derivatives on colon cancer cells. *Acta Biochim. Biophys. Sin.* **2015**, *47*, 824–833. [CrossRef]
8. Jantova, S.; Cipak, L.; Letasiova, S. Berberine induces apoptosis through a mitochondrial/caspase pathway in human promonocytic U937 cells. *Toxicol. In Vitro* **2007**, *21*, 25–31. [CrossRef]
9. Tian, Y.; Zhao, L.; Wang, Y.; Zhang, H.; Xu, D.; Zhao, X.; Li, Y.; Li, J. Berberine inhibits androgen synthesis by interaction with aldo-keto reductase 1C3 in 22Rv1 prostate cancer cells. *Asian J. Androl.* **2016**, *18*, 607–612.
10. Lu, J.J.; Fu, L.; Tang, Z.; Zhang, C.; Qin, L.; Wang, J.; Yu, Z.; Shi, D.; Xiao, X.; Xie, F.; et al. Melatonin inhibits AP-2beta/hTERT, NF-kappaB/COX-2 and Akt/ERK and activates caspase/Cyto C signaling to enhance the antitumor activity of berberine in lung cancer cells. *Oncotarget* **2016**, *7*, 2985–3001.
11. Wang, J.; Qi, Q.; Feng, Z.; Zhang, X.; Huang, B.; Chen, A.; Prestegarden, L.; Li, X.; Wang, J. Berberine induces autophagy in glioblastoma by targeting the AMPK/mTOR/ULK1-pathway. *Oncotarget* **2016**, *7*, 66944–66958. [CrossRef]
12. Mishan, M.A.; Ahmadiankia, N.; Matin, M.M.; Heirani-Tabasi, A.; Shahriyari, M.; Bidkhori, H.R.; Naderi-Meshkin, H.; Bahrami, A.R. Role of Berberine on molecular markers involved in migration of esophageal cancer cells. *Cell. Mol. Biol.* **2015**, *61*, 37–43.
13. Chen, Q.; Qin, R.; Fang, Y.; Li, H. Berberine sensitizes human ovarian cancer cells to cisplatin through miR93/PTEN/Akt signaling pathway. *Cell Physiol. Biochem.* **2015**, *36*, 956–965. [CrossRef]

14. Chen, K.; Li, G.; Geng, F.; Zhang, Z.; Li, J.; Yang, M.; Dong, L.; Gao, F. Berberine reduces ischemia/reperfusion-induced myocardial apoptosis via activating AMPK and PI3K-Akt signaling in diabetic rats. *Apoptosis* **2014**, *19*, 946–957. [CrossRef]

15. Li, L.; Wang, X.; Sharvan, R.; Gao, J.; Qu, S. Berberine could inhibit thyroid carcinoma cells by inducing mitochondrial apoptosis, G_0/G_1 cell cycle arrest and suppressing migration via PI3K-AKT and MAPK signaling pathways. *Biomed. Pharmacother.* **2017**, *95*, 1225–1231. [CrossRef]

16. Li, F.; Dong, X.; Lin, P.; Jiang, J. Regulation of Akt/FoxO3a/Skp2 Axis is critically involved in berberine-induced cell cycle arrest in hepatocellular carcinoma cells. *Int. J. Mol. Sci.* **2018**, *19*, 327.

17. Eo, S.H.; Kim, J.H.; Kim, S.J. Induction of G_2/M arrest by berberine via activation of PI3K/Akt and p38 in human chondrosarcoma cell line. *Oncol. Res.* **2014**, *22*, 147–157. [CrossRef]

18. Park, S.H.; Sung, J.H.; Kim, E.J.; Chung, N. Berberine induces apoptosis via ROS generation in PANC-1 and MIA-PaCa2 pancreatic cell lines. *Braz. J. Med. Biol. Res.* **2015**, *48*, 111–119. [CrossRef]

19. Gu, M.; Xu, J.; Han, C.; Kang, Y.; Liu, T.; He, Y.; Huang, Y.; Liu, C. Effects of berberine on cell cycle, DNA, reactive oxygen species, and apoptosis in L929 murine fibroblast cells. *Evid. Based Complement. Alternat. Med.* **2015**, *2015*, 796306. [CrossRef]

20. Jantova, S.; Letasiova, S.; Brezova, V.; Cipak, L.; Labaj, J. Photochemical and phototoxic activity of berberine on murine fibroblast NIH-3T3 and Ehrlich ascites carcinoma cells. *J. Photochem. Photobiol. B* **2006**, *85*, 163–176. [CrossRef]

21. Wang, L.; Liu, L.; Shi, Y.; Cao, H.; Chaturvedi, R.; Calcutt, M.W.; Hu, T.; Ren, X.; Wilson, K.T.; Polk, D.B.; et al. Berberine induces caspase-independent cell death in colon tumor cells through activation of apoptosis-inducing factor. *PLoS ONE* **2012**, *7*, e36418. [CrossRef]

22. Jung-Mu, H.; Mee-Sun, H.; Sang-Yong, L.; Woo-Yiel, L.; Dongho, K. The combination of berberine and irradiation enhances anti-cancer effects via activation of p38 MAPK pathway and ROS generation in human hepatoma cells. *J. Cell. Biochem.* **2009**, *107*, 955–964.

23. Tong, N.; Zhang, J.; Chen, Y.; Zhubo, L.I.; Luo, Y.; Zuo, H.; Zhao, X. Berberine sensitizes mutliple human cancer cells to the anticancer effects of doxorubicin in vitro. *Oncol. Lett.* **2012**, *3*, 1263–1267. [CrossRef]

24. Zhao, Y.; Jing, Z.; Li, Y.; Mao, W. Berberine in combination with cisplatin suppresses breast cancer cell growth through induction of DNA breaks and caspase-3-dependent apoptosis. *Oncol. Rep.* **2016**, *36*, 567–572. [CrossRef]

25. Zheng, F.; Wu, J.; Tang, Q.; Xiao, Q.; Wu, W.; Hann, S.S. The enhancement of combination of berberine and metformin in inhibition of DNMT1 gene expression through interplay of SP1 and PDPK1. *J. Cell Mol. Med.* **2018**, *22*, 600–612. [CrossRef]

26. Halicka, H.D.; Garcia, J.; Li, J.; Zhao, H.; Darzynkiewicz, Z. Synergy of 2-deoxy-d-glucose combined with berberine in inducing the lysosome/autophagy and transglutaminase activation-facilitated apoptosis. *Apoptosis* **2017**, *22*, 229–238. [CrossRef]

27. Pandey, A.; Vishnoi, K.; Mahata, S.; Tripathi, S.C.; Misra, S.P.; Misra, V.; Mehrotra, R.; Dwivedi, M.; Bharti, A.C. Berberine and curcumin target survivin and STAT3 in gastric cancer cells and synergize actions of standard chemotherapeutic 5-fluorouracil. *Nutr. Cancer* **2015**, *67*, 1293–1304. [CrossRef] [PubMed]

28. Gong, J.; Munoz, A.R.; Pingali, S.; Payton-Stewart, F.; Chan, D.E.; Freeman, J.W.; Ghosh, R.; Kumar, A.P. Downregulation of STAT3/NF-kappaB potentiates gemcitabine activity in pancreatic cancer cells. *Mol. Carcinog.* **2017**, *56*, 402–411. [CrossRef]

29. Yang, X.L.; Huang, N. Berberine induces selective apoptosis through the AMPK-mediated mitochondrial/caspase pathway in hepatocellular carcinoma. *Mol. Med. Rep.* **2013**, *8*, 505–510. [CrossRef]

30. Liu, B.; Wang, G.S.; Yang, J.; Pan, X.D.; Yang, Z.C.; Zang, L.Q. Berberine inhibits human hepatoma cell invasion without cytotoxicity in healthy hepatocytes. *PLoS ONE* **2011**, *6*, e21416. [CrossRef]

31. Liu, C.S.; Zheng, Y.R.; Zhang, Y.F.; Long, X.Y. Research progress on berberine with a special focus on its oral bioavailability. *Fitoterapia* **2016**, *109*, 274–282. [CrossRef]

32. Cui, H.X.; Hu, Y.N.; Li, J.W.; Yuan, K.; Guo, Y. Preparation and evaluation of antidiabetic agents of berberine organic acid salts for enhancing the bioavailability. *Molecules* **2018**, *24*, 103. [CrossRef]

33. Hsu, H.K.; Hsu, K.H.; Cheng, Y.M.; Suen, H.Y.; Peng, S.F. Development and in vitro evaluation of linear PEI-shelled heparin/berberine nanoparticles in human osteosarcoma U-2 OS cells. *Molecules* **2018**, *23*, 3122. [CrossRef]

34. Huang, Z.J.; Zeng, Y.; Lan, P.; Sun, P.H.; Chen, W.M. Advances in structural modifications and biological activities of berberine: An active compound in traditional Chinese medicine. *Mini Rev. Med. Chem.* **2011**, *11*, 1122–1129. [CrossRef]

35. Lo, C.Y.; Hsu, L.C.; Chen, M.S.; Lin, Y.J.; Chen, L.G.; Kuo, C.D.; Wu, J.Y. Synthesis and anticancer activity of a novel series of 9-O-substituted berberine derivatives: A lipophilic substitute role. *Bioorg. Med. Chem. Lett.* **2013**, *23*, 305–309. [CrossRef]

36. Zhang, S.; Wang, X.; Yin, W.; Liu, Z.; Zhou, M.; Xiao, D.; Liu, Y.; Peng, D. Synthesis and hypoglycemic activity of 9-O-(lipophilic group substituted) berberine derivatives. *Bioorg. Med. Chem. Lett.* **2016**, *26*, 4799–4803. [CrossRef]

37. Li, R.; Wu, J.; He, Y.; Hai, L.; Wu, Y. Synthesis and in vitro evaluation of 12-(substituted aminomethyl) berberrubine derivatives as anti-diabetics. *Bioorg. Med. Chem. Lett.* **2014**, *24*, 1762–1765. [CrossRef]

38. Zou, K.; Li, Z.; Zhang, Y.; Zhang, H.Y.; Li, B.; Zhu, W.L.; Shi, J.Y.; Jia, Q.; Li, Y.M. Advances in the study of berberine and its derivatives: A focus on anti-inflammatory and anti-tumor effects in the digestive system. *Acta Pharmacol. Sin.* **2017**, *38*, 157–167. [CrossRef]

39. Jin, X.; Song, X.; Cao, Y.B.; Jiang, Y.Y.; Sun, Q.Y. Research progress in structural modification and pharmacological activities of berberine. *J. Pharma Prac.* **2014**, *32*, 171–175.

40. Xiao, D.; He, F.; Peng, D.; Zou, M.; Peng, J.; Liu, P.; Liu, Y.; Liu, Z. Synthesis and anticancer activity of 9-O-pyrazole alkyl substituted berberine derivatives. *Anticancer Agents Med. Chem.* **2018**, *18*, 1639–1648. [CrossRef]

41. Xiong, Y.-X.; Su, H.F.; Lv, P.; Ma, Y.; Wang, S.K.; Miao, H.; Huang, Z.S. A newly identified berberine derivative induces cancer cell senescence by stabilizing endogenous G-quadruplexes and sparking a DNA damage response at the telomere region. *Oncotarget* **2015**, *6*, 35625–35635. [CrossRef] [PubMed]

42. Liu, Z.; Wang, X.; Zhang, H.; Zhang, S.; Li, Y.; Liu, Y.; Peng, D. Synthesis and anti-inflammatory effects of a series of novel 9-O-substituted berberine derivatives. *Med. Chem. Res.* **2017**, *26*, 672–679. [CrossRef]

43. Xiao, D.; Liu, Z.; Zhang, S.; Zhou, M.; He, F.; Zou, M.; Peng, J.; Xie, X.; Liu, Y.; Peng, D. Berberine derivatives with different pharmacological activities via structural modifications. *Mini Rev. Med. Chem.* **2018**, *18*, 1424–1441. [CrossRef] [PubMed]

44. Jin, Y.; Khadka, D.B.; Cho, W.J. Pharmacological effects of berberine and its derivatives: A patent update. *Expert Opin. Ther. Pat.* **2016**, *26*, 229–243. [CrossRef] [PubMed]

45. Kłosińska-Szmurło, E.; Pluciński, F.A.; Grudzień, M.; Betlejewska-Kielak, K.; Biernacka, J.; Mazurek, A.P. Experimental and theoretical studies on the molecular properties of ciprofloxacin, norfloxacin, pefloxacin, sparfloxacin, and gatifloxacin in determining bioavailability. *J. Biol. Phys.* **2014**, *40*, 335–345. [CrossRef]

46. Sharma, P.C.; Jain, A.; Jain, S.; Pahwa, R.; Yar, M.S. Ciprofloxacin: Review on developments in synthetic, analytical, and medicinal aspects. *J. Enzyme Inhib. Med. Chem.* **2010**, *25*, 577–589. [CrossRef] [PubMed]

47. Zhou, X.Y.; Ye, X.G.; He, L.T.; Zhang, S.R.; Wang, R.L.; Zhou, J.; He, Z.S. In vitro characterization and inhibition of the interaction between ciprofloxacin and berberine against multidrug-resistant Klebsiella pneumoniae. *J. Antibiot.* **2016**, *69*, 741–746. [CrossRef] [PubMed]

48. Man, S.; Potacek, M.; Necas, M.; Zak, Z.; Dostal, J. Molecular and crystal structures of three berberine derivatives. *Molecules* **2001**, *6*, 433–441. [CrossRef]

49. Das, B.; Srinivas, K.V.N.S. Conversion of berberine into berberrubine by selective demethylation under microwave irradiation. *Synth. Commun.* **2002**, *32*, 3027–3029. [CrossRef]

50. Delgado-Camon, A.; Jarne, C.; Cebolla, V.L.; Larrañaga, O.; de Cozar, A.; Cossio, F.P.; Vara, Y.; Dominguez, A.; Membrado, L.; Galban, J.; et al. Resonance driven regioselective demethylation of berberine. Microwave assisted synthesis of berberrubine and its assessment as fluorescent chemosensor for alkanes. *Tetrahedron* **2015**, *71*, 6148–6154. [CrossRef]

51. Shaikh, A.R.; Patel, N.B.; Rajani, D. Antimycobacterial and antimicrobial studies of newly synthesized 3-(4-(6-methylbenzo[d]thiazol-2-yl) phenyl)quinazolin-4(3H)-ones. *Indian J. Res. Pharm. Biotechnol.* **2014**, *2*, 935–942.

52. Tomisic, Z.B.; Kujundzic, N.K.; Bukvic Krajacic, M.; Visnjevac, A.; Kojic-Prodic, B. Molecular structures of new ciprofloxacin derivatives. *J. Mol. Struct.* **2002**, *611*, 73–81. [CrossRef]

53. Hassan, H.M.A.; Harakeh, S.; Sakkaf, K.A.; Denetiu, I. Progress in microwave-aided chemical synthesis. *Australian J. Chem.* **2012**, *65*, 1647–1654. [CrossRef]

54. Han, X.; Shao, K.; Hu, W. Synthesis of 9-substituted berberine derivatives with microwave irradiation. *Chem. Res. Chin. Univ.* **2018**, *34*, 571–577. [CrossRef]

55. Inbaraj, J.J.; Kukielczak, B.M.; Bilski, P.; Sandvik, S.L.; Chignell, C.F. Photochemistry and photocytotoxicity of alkaloids from Goldenseal (*Hydrastis canadensis* L.) 1. Berberine. *Chem. Res. Toxicol.* **2001**, *14*, 1529–1534. [CrossRef] [PubMed]

56. Hirakawa, K.; Hirano, T.; Nishimura, Y.; Arai, T.; Nosaka, Y. Dynamics of singlet oxygen generation by DNA-binding photosensitizers. *J. Phys. Chem. B* **2012**, *116*, 3037–3044. [CrossRef] [PubMed]

57. Hirakawa, K.; Hirano, T. The microenvironment of DNA switches the activity of singlet oxygen generation photosensitized by berberine and palmatine. *Photochem. Photobiol.* **2008**, *84*, 202–208. [CrossRef] [PubMed]

58. Zalibera, M.; Rapta, P.; Stasko, A.; Brindzova, L.; Brezova, V. Thermal generation of stable spin trap adducts with super-hyperfine structure in their EPR spectra: An alternative EPR spin trapping assay for radical scavenging capacity determination in dimethylsulphoxide. *Free Radic. Res.* **2009**, *43*, 457–469. [CrossRef]

59. Landolt, H.; Börnstein, R.; Fischer, H.; Madelung, O.; Deuschle, G. *Landolt-Börnstein, Numerical Data and Functional Relationships in Science and Technology*; Springer: Berlin/Heidelberg, Germany, 1987; Volume 17, pp. 35–249.

60. Marshall, D.L.; Christian, M.L.; Gryn'ova, G.; Coote, M.L.; Barker, P.J.; Blanksby, S.J. Oxidation of 4-substituted TEMPO derivatives reveals modifications at the 1- and 4-positions. *Org. Biomol. Chem.* **2011**, *9*, 4936–4947. [CrossRef]

61. Mossmann, T. Rapid colorimetric assay for cellular growth and survival: Application to proliferation and cytotoxicity assays. *J. Immunol. Methods* **1983**, *65*, 55–63. [CrossRef]

62. Majno, G.; Joris, I. Apoptosis, oncosis, and necrosis. An overview of cell death. *Am. J. Pathol.* **1995**, *146*, 3–15. [PubMed]

63. Fujita, K.; Iwama, H.; Oura, K.; Tadokoro, T.; Samukawa, E.; Sakamoto, T.; Nomura, T.; Tani, J.; Yoneyama, H.; Morishita, A.; et al. Cancer therapy due to apoptosis: Galectin-9. *Int. J. Mol. Sci.* **2017**, *18*, 74. [CrossRef]

64. Stoll, S.; Schweiger, A. EasySpin, a comprehensive software package for spectral simulation and analysis in EPR. *J. Magn. Reson.* **2006**, *178*, 42–55. [CrossRef] [PubMed]

65. Jantova, S.; Paulovicova, E.; Paulovicova, L.; Topolska, D.; Panik, M.; Milata, V. Assessment of immunomodulatory activities and in vitro toxicity of new quinolone 7-ethyl-9-ethyl-6-oxo-6,9-dihydro [1,2,5]selenadiazolo[3,4-h]quinoline-7-carboxylate. *Immunol. Investig.* **2017**, *46*, 341–360. [CrossRef]

66. Cipak, L.; Rauko, P.; Miadokova, E.; Cipakova, I.; Novotny, L. Effects of flavonoids on cisplatin-induced apoptosis of HL-60 and L1210 leukemia cells. *Leuk. Res.* **2003**, *27*, 65–72. [CrossRef]

67. Cipak, L.; Novotny, L.; Cipakova, I.; Rauko, P. Differential modulation of cisplatin and doxorubicin efficacies in leukemia cells by flavonoids. *Nutr. Res.* **2003**, *8*, 1045–1057. [CrossRef]